The Effect of "Skin-Core" Morphology on the Heat-Deflection Temperature of Polypropylene

D. JARUS,[1] A. SCHEIBELHOFFER,[2] A. HILTNER,[1,*] and E. BAER[1]

[1]Department of Macromolecular Science and Center for Applied Polymer Research, Case Western Reserve University, Cleveland, Ohio 44106; [2]Ferro Corporation, 7500 E. Pleasant Valley Rd., Independence, Ohio 44131

SYNOPSIS

The relationship between solid-state morphology and heat-deflection temperature (HDT) of nucleated polypropylenes was studied. Using optical microscopy to characterize the morphology and DMTA to determine the temperature dependence of the tensile modulus, a composite model was adapted to estimate the HDT. Both compression-molded films and injection-molded HDT bars were investigated. Compression-molded films were isotropic except for a thin skin, and the temperature dependence of the tensile modulus was very similar for all compression-molded films regardless of the nucleating agent. Results on isotropic specimens could not account for the higher ASTM HDT of nucleated samples. Injection-molded HDT bars exhibited an anisotropic gradient in both the morphology and the temperature-dependent modulus. A composite model was developed to estimate the HDT. The model successfully predicted the ASTM HDT values relative to the HDT of unnucleated polypropylene. The increase in HDT was caused by the increased retention of melt orientation, due, in turn, to the higher crystallization temperature of the nucleated samples. © 1996 John Wiley & Sons, Inc.

INTRODUCTION

The heat-deflection temperature (HDT) is frequently used as an indicator of the practical use temperature of thermoplastics. The HDT, defined by ASTM D 648, is the temperature at which a specimen deflects 0.25 mm under a designated outer fiber stress. The HDT is not necessarily an intrinsic property of a material. Values of the HDT depend upon the processing conditions such as the melt temperature and mold temperature and also upon nucleating agents which alter the crystallization kinetics of the material. For example, addition of nucleating agents to polypropylene can increase the HDT by over 15°C.[1] These differences may be related to the process-induced morphology. An attempt was made to relate the orientation at the center of an injection-molded bar to the HDT; however, a correlation is not directly evident.[1] Injection-molded polypropylene has a gradient morphology through the cross section, and structural characteristics measured at the center may not be representative of the entire specimen. Other physical properties of polypropylene such as Izod impact strength, tensile behavior, and modulus differ across the morphology gradient of injection-molded specimens.[2] The composite modulus of injection-molded polypropylene has been shown to be an additive function of the "skin–core" structure.[3] It is anticipated that this gradient also affects the HDT, since the HDT is determined by the temperature dependence of the flexural modulus. The aim of this work was to investigate the morphological gradient of polypropylene and relate the gradient solid-state structure to the HDT. Different nucleating agents were added to vary the solid-state structure under identical processing conditions.

EXPERIMENTAL

Polypropylene (Shell 5A64) was compounded with a commercial nucleating agent, talc, or peroxide at 0.20–0.25% by weight. The compounded samples are

* To whom correspondence should be addressed.

Journal of Applied Polymer Science, Vol. 60, 209–219 (1996)
 CCC 0021-8995/96/020209-11

referred to as PP, PP-Md, PP-Tc, and PP-Px. The additives are described in Table I. Each composition, including the virgin resin, was run through a Werner Pfliderer ZSK-30 twin-screw extruder to ensure mixing and pelletized. The pellets were injection-molded into ASTM D 648 heat-deflection bars on a 40 ton Newburry injection-molding machine. The barrel and mold temperatures were 200 and 40°C, respectively. The back pressure was 250 psi. Pellets were also compression-molded into thin (400 μm) films. The films were prepared by premelting the pellets for 10 min at 200°C, compressing for 10 min at 15,000 lb ram force, and cooling to room temperature at ca. 15°C/min.

HDTs were measured on the injection-molded bars (3 × 13 mm) under an outer fiber stress of 66 psi. In all instances, the ASTM standard was followed.[7]

Melting and crystallization behavior were determined with a Perkin-Elmer differential scanning calorimeter (DSC) 7. A dry ice/ethanol slurry was used as the coolant and nitrogen was used as the purge gas. The instrument was calibrated with indium and tin standards. Heating, cooling, and second heating scans of pellets were recorded at 10°C/min over the temperature range of 30–200°C, with 3-min hold at the end of each scan.

Thin cross sections, approximately 1 μm thick, were cut using an RMC MT6000XL ultramicrotome. The sections were taken from the center of the compression moldings. In the case of the injection-molded bars, the sections were cut from the center of the bar in the longitudinal direction. The thin sections were examined under cross polars in an Olympus BH-2 transmission optical microscope. Due to the anisotropy of the injection-molded specimens, photographs were taken at several cross polar angles. The average chain axis orientation was determined by inserting a 530 nm wave length (first order) birefringent plate between the sample and the analyzer. The average chain axis orientation was taken as the slow axis of the birefringent plate when the retardance was at a maximum. The degree of orientation was qualitatively taken as the intensity of the light viewed through cross polars.

The tensile modulus was measured as a function of temperature in a Polymer Labs Mark II dynamic mechanical thermal analyzer (DTMA). The samples were tested at a frequency of 1 Hz. The modulus measurements were made from room temperature to 160°C at a heating rate of 2°C/min. Specimens roughly 40 × 8 cm were cut from the compression-molded films for testing. In the case of the injection-molded specimens, sections approximately 400 μm thick were cut from the bars at several positions through the thickness as determined by the microscopy. The sections were cut with a diamond wafering blade on a Buelher Isomet low-speed cutting saw. The sections were taken approximately midway between the ends of the bar. They were approximately the same dimensions as those cut from compression-molded films. For sections near the mold surface, the surface was polished off to the desired depth on a Buehler Metaserv grinder/polisher. Water was used as a coolant for both cutting and polishing. The 40 cm-long specimens were tested in tension with a gauge length of 25 cm. Storage and loss modulus were recorded.

RESULTS AND DISCUSSION

Thermal Characterization

The cooling thermograms in Figure 1 compare the crystallization behavior of the four samples. The crystallization peak temperatures ranged from a low of 113°C for PP-Px to a high of 128°C for PP-Md.

Table I Sample Designations and Additives to Polypropylene

Sample Designation	Additive[a]				
	Trade Name	Weight %	Form	Structure	Function
PP	None	—	—	—	—
PP-Px	CR-05	0.25	Pellet	2,5-Dimethyl-2,5-di(*t*-butylperoxy)hexane	Flow modifier and processing aid
PP-Tc	Vantalc 6h	0.20	Powder	Platelike talc particles, median diameter, 2.3 μm	Nucleating agent
PP-Md	Millad 3940	0.25	White powder	A benzylidene sorbitol	Commercial nucleating agent

[a] Refs. 4–6.

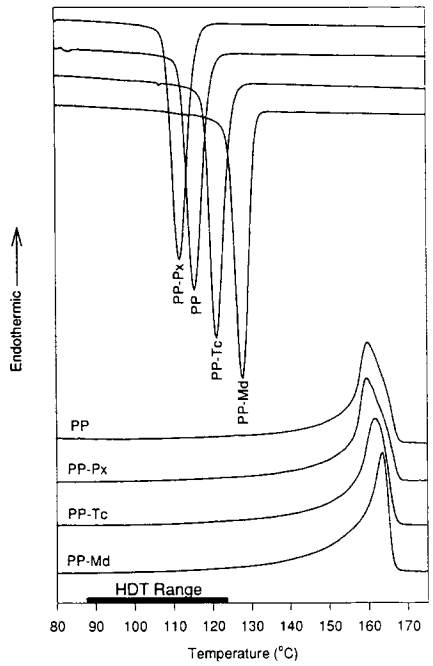

Figure 1 Crystallization and subsequent melting thermograms of polypropylene samples. Scanning rate is 10°C/min.

Millad most effectively nucleated the polypropylene; however, talc also acted as a nucleating agent as seen by the increase in crystallization temperature from 116°C for PP to 121°C for PP-Tc. Peroxide "denucleated" polypropylene, as indicated by a decrease in the peak temperature from 116°C for PP to 113°C for PP-Px. The shape of the crystallization exotherm was determined primarily by the kinetics of crystal growth. The exotherms of PP, PP-Px, and PP-Tc had similar shapes and, hence, similar crystallization kinetics. The sharper crystallization peak of PP-Md indicated that, in addition to nucleating polypropylene, Millad also increased the crystallization rate.

The subsequent melting thermograms are presented below in Figure 1. In all the samples, melting began at approximately 100°C and a long shoulder extended to the melting peak. Melting started in the range of the HDT, although the extent of melting in this range was minimal. Most of the melting occurred above 150°C. There were slight differences in the shapes of the melting endotherms. The PP and PP-Px endotherms had the lowest peak temperature of 160°C, with an indication of a higher temperature shoulder. The PP-Tc endotherm had a higher peak temperature of 162°C and there was no indication of the shoulder. The PP-Md endotherm had the highest peak temperature of 165°C, and the sharp melting peak had a low-temperature shoulder. The nucleated samples exhibited a slightly higher degree of crystallinity than that of the control and PP-Px (Table II).

Compression-molded Samples

Morphology

Typical regions of the cross section of thin (400–500 μm) compression-molded films are depicted in Figure 2. There were no morphological variations through the film thickness, except for a very thin 10–15 μm skin (not shown). The spherulitic texture varied from sample to sample. The fineness of the texture correlated with the crystallization temperature, i.e., the higher the crystallization temperature, the higher the nucleation density and the finer the texture. As is typical for polypropylene, PP had type I spherulites with an occasional type III spherulite, identifiable by its high birefringence (not shown). The average spherulite size was 15–20 μm. The spherulites of PP-Px were similar to those of PP; however, the average spherulitic size, 40–50 μm, was much larger than in PP. Nucleation of polypropylene by talc produced small, poorly defined spherulites,

Table II Crystallinity, Modulus, and HDT Values of Polypropylene Materials

	Crystallinity[a] (%)	E' at 25°C[b] (GPa)	E' at 100°C[b] (MPa)	Measured HDT[c] (n = 6) (°C)	Literature HDT[c,d] (°C)	Calculated HDT (°C)
PP	47	1.8	490	96 ± 3.0	108	116
PP-Px	47	1.8	490	93 ± 1.5	N/A	113
PP-Tc	49	2.0	500	108 ± 3.0	121	122
PP-Md	50	2.1	530	107 ± 4.5	123	124

[a] Assuming ΔH_f = 209 J/g.[8]
[b] Compression-molded films.
[c] ASTM D 648.
[d] Ref. 1.

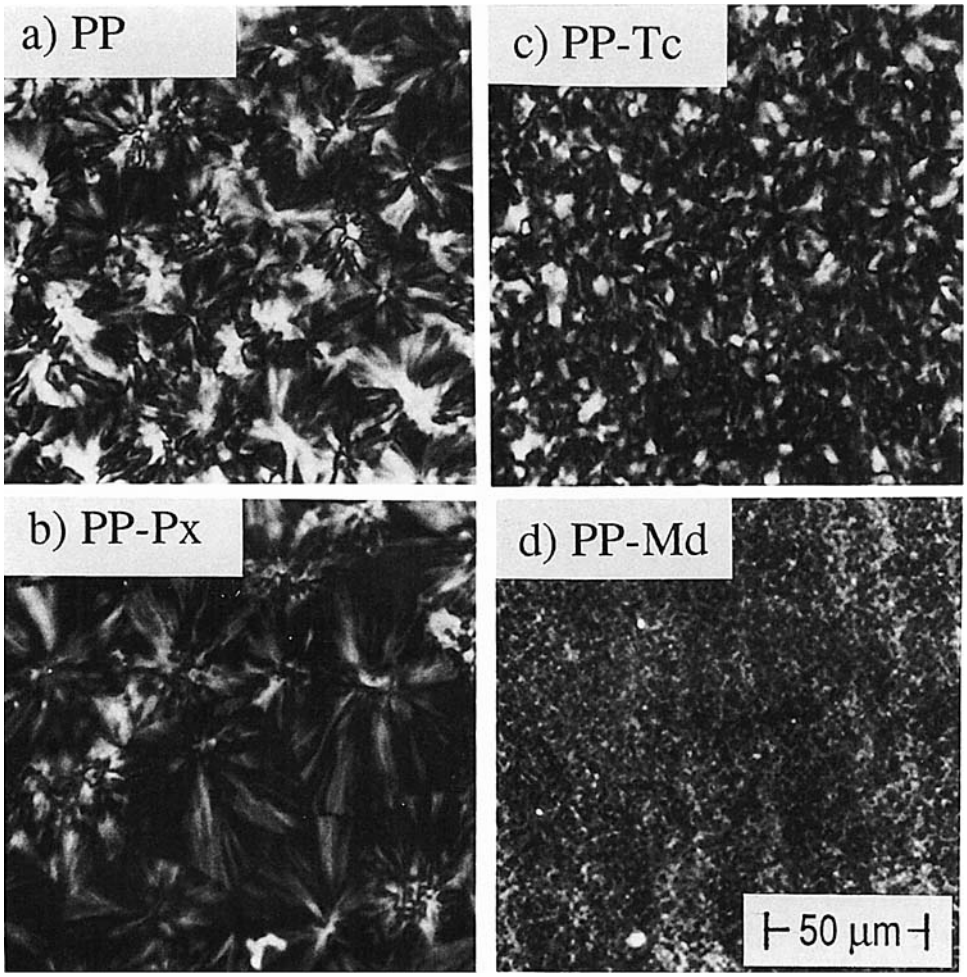

Figure 2 Optical micrographs of compression-molded films. Sections shown are 1 μm thick. The lines are knife marks.

as was observed previously.[9] In PP-Md, the texture was so fine that individual spherulites were indistinguishable.

Modulus Measurements

Figure 3 shows the modulus of thin compression-molded films from room temperature (RT) to 160°C, almost to the melt. The RT modulus of the nucleated samples, PP-Md and PP-Tc, was significantly higher than the RT modulus of the PP control and PP-Px (Table II). The higher RT modulus of the nucleated samples correlated with the slightly higher crystallinity. As the temperature increased into the range of the HDT, the modulus differences among the samples diminished, so that at 100°C PP, PP-Px, and PP-Tc had essentially the same value and PP-Md had a modulus only slightly higher than the others (Table II).

Estimation of Heat Deflection Temperature

The HDT test was simulated by a calculation of the temperature-dependent deflection in a three-point bend. For the geometry specified by the HDT test, the shear contribution (roughly 6%) could not be neglected. Assuming an elastic bar, the deflection as a function of temperature in a three-point bend, $D(T)$, including the shear contribution, is given by

$$D(T) = \frac{PL^3}{48E(T)I}\left[1 + \left(\frac{h}{2L}\right)^2 \frac{E(T)}{G(T)}\right] \quad (1)$$

where P, the load, is $1.53N$; L, the length between loading points, is 100 mm; $E(T)$ and $G(T)$ are the Young's modulus and the shear modulus at temperature T, respectively; h, the height of the bar, is 13 mm; b, the width of the bar, is 3 mm; and I, the moment of inertia, equals bh^3. A Poisson's ratio of

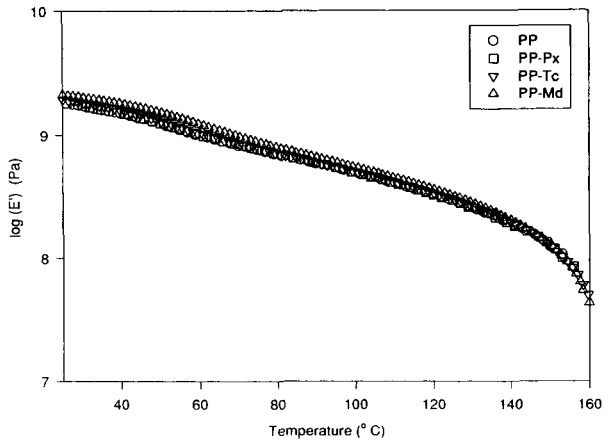

Figure 3 Temperature dependence of the modulus of compression-molded samples determined by DMTA at 1 Hz.

0.45 for PP was assumed to estimate $G(T)$ from $E(T)$. The ASTM test stipulates that the specimen be loaded for 5 min before the test begins. The deflection is then set to zero and the test started.[7] Therefore, in the calculations, it was necessary to subtract the deflection at RT:

$$\mathcal{D}(T) = D(T) - D(\mathrm{RT}) \qquad (2)$$

A correction was also made to the temperature axis to account for time effects. To estimate the temperature shift between the modulus data obtained at 1 Hz and an effective frequency of 10^{-3} Hz, assumed for the static HDT test, the activation energy of the glass transition, 117 kJ/mol, was used.[10] The use of the activation energy of the alpha relaxation would have been more appropriate in this temperature range; however, this was difficult to obtain due to the breadth of the alpha relaxation. With the estimated 15°C shift in the temperature axis, the calculated deflection is plotted Figure 4. The HDT condition, $\mathcal{D}(T) = 250$ μm, is given as the dashed line. The calculated HDT is quite similar for all four samples. Differences in the RT modulus values had little effect on the HDT, as little or no deflection occurred at this temperature. The calculated deflection depended more upon the high-temperature modulus. The modulus values at 25 and 100°C are listed in Table I. Since the high-temperature modulus values were all similar, the calculated HDT was also very similar. This was not consistent with the measured values, where a spread of 14°C was seen (Table I). However, the measured ASTM values were obtained on injection-molded specimens where processing produced gradient morphologies that were not present in the compression-molded films used for modulus measurements.

Injection-molded Samples

Morphology of Injection-molded Polypropylene

Cross sections from the surface to the center of the injection-molded HDT test bars are shown in Figure 5(a)–(d). The sections were cut parallel to the injection direction and the micrographs were taken with the crossed polars at 0°, 15°, 25°, and 45° to the injection direction. The gradient structure from the edge to the center is described as five layers, designated I–V. A schematic of the layers is presented below the micrographs. The direction of the lines in the schematic represents the chain orientation and the density of the lines indicates the degree of orientation.

The layered structure of PP is shown in Figure 5(a). At the surface, Layer I, approximately 135 μm thick, is nonspherulitic and highly oriented with the chain axis parallel to the injection direction. Layer II is spherulitic and approximately 85 μm thick. The chain orientation is shifted roughly 5°–10° from the injection direction. Layer III is also spherulitic and 70 μm thick. It shows no preferred chain orientation from cross polars, and only very faint orientation with the birefringent plate inserted. Layer IV, extending another 625 μm, shows a gradient in orientation as seen by the shift in birefringence as the crossed polars are rotated. The region closest to the surface favors an orientation of 45°, whereas the inner region favors an orientation almost parallel to the injection direction. Layer V is the spherulitic core and extends another 585 μm to the center of

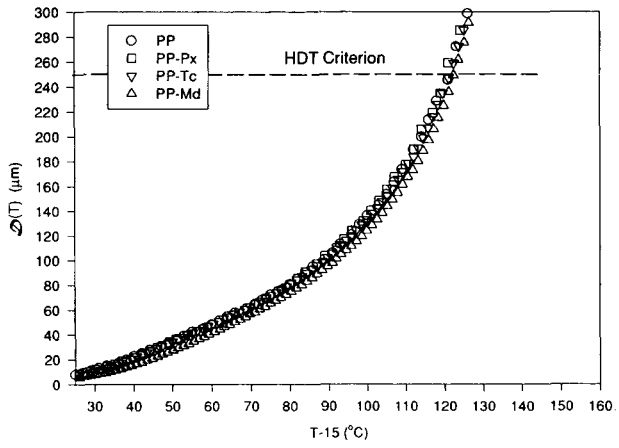

Figure 4 Calculated deflection as a function of temperature using compression-molded modulus values. HDT criterion given at 250 μm.

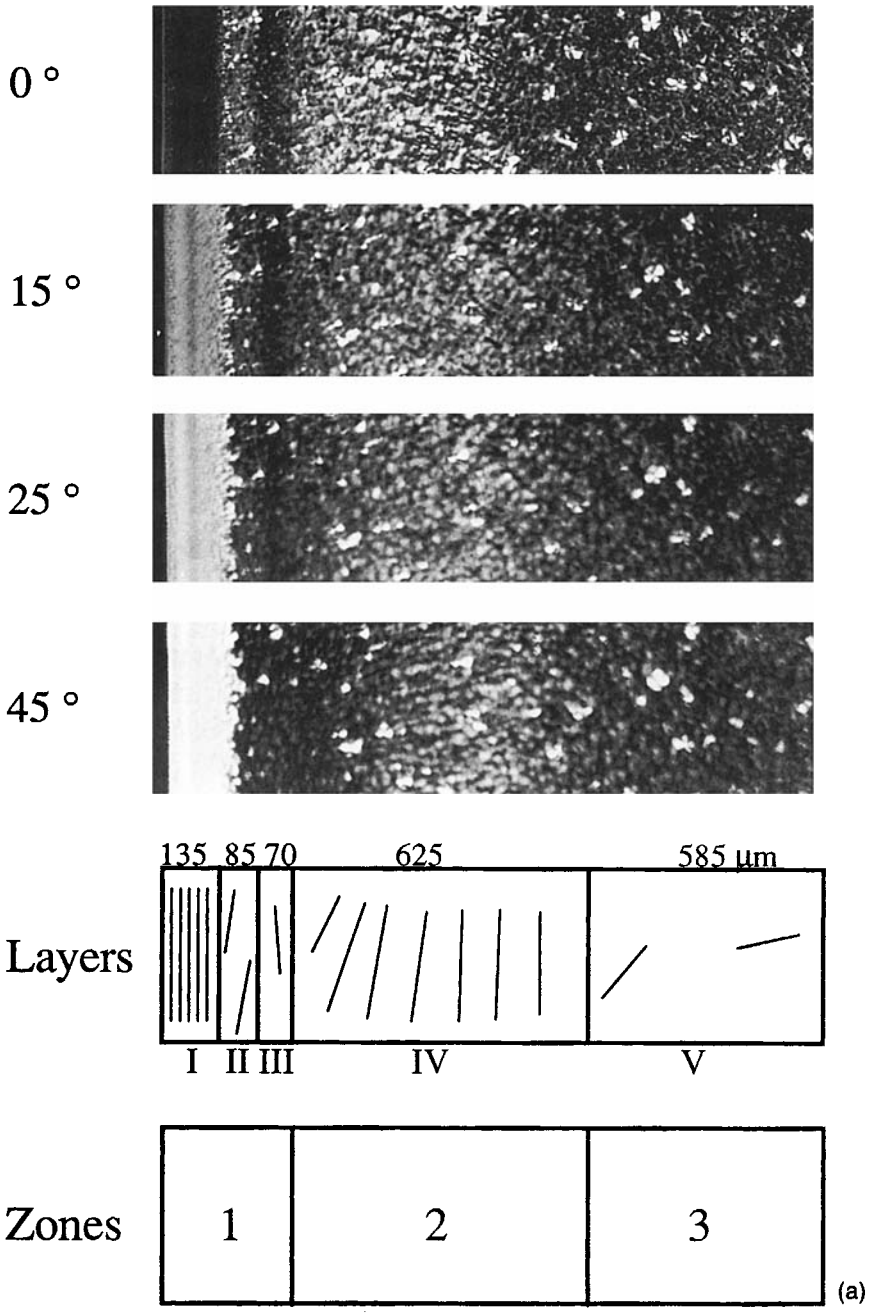

Figure 5 Optical micrographs and schematics of the cross section of injection-molded HDT bars. The micrograph is from the edge to the center of the specimen. Crossed polar angles are indicated next to the micrographs: (a) PP; (b) PP-Px; (c) PP-Tc; (d) PP-Md.

the sample. This layer does not exhibit any anisotropy under cross-polarized light, but does show a very faint orientation with the birefringent plate inserted.

The morphology of injection-molded semicrystalline polymers depends upon the orientation incurred in the melt during mold filling and the extent of relaxation before crystallization as the melt cools. Orientation achieved by extensional flow at the fountain flow front affects the outer layers of the sample. Shear forces due to the velocity gradient in the mold filling flow behind the flow front control orientation in the center of the sample. The shear forces are zero at the edge of the solidified outer layers and the center with a maximum in between.[11,12]

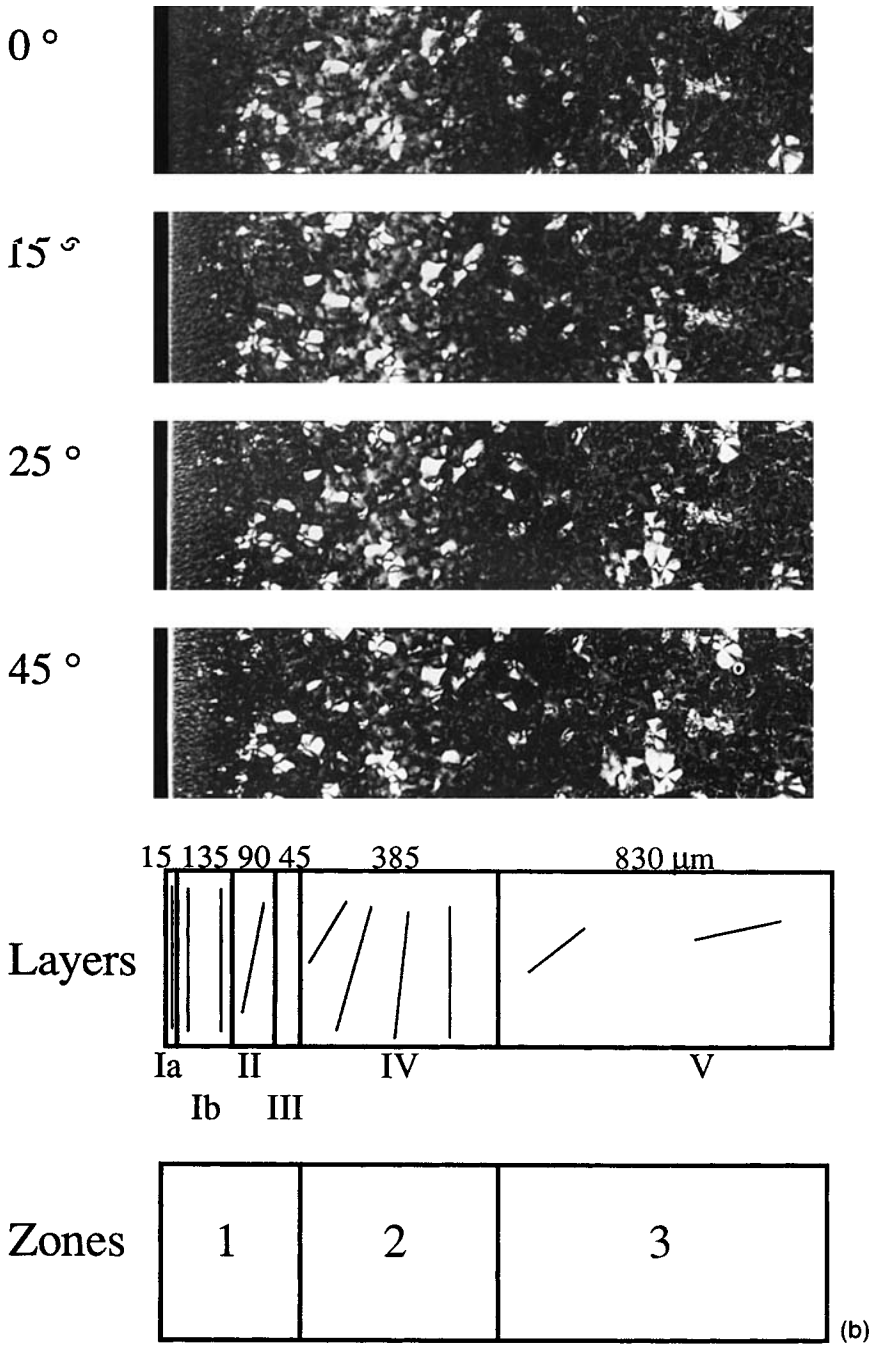

Figure 5 (*Continued from the previous page*)

Layers I and II come from the fountain flow front. Very rapid cooling at the mold wall produces a highly oriented skin, Layer I, which retains most of the melt orientation. Layer II cools more slowly than Layer I so that some of the orientation relaxes and there is also time for spherulites to nucleate and grow. The extensional fountain flow meets the oncoming shear flow in Layer III. As a consequence of the opposing flows, this is a region with very little orientation. The material in Layers IV and V comes from the mold filling. Layer IV is closer to the mold surface and crystallizes before Layer V; consequently, it retains more of the melt orientation than does Layer V.

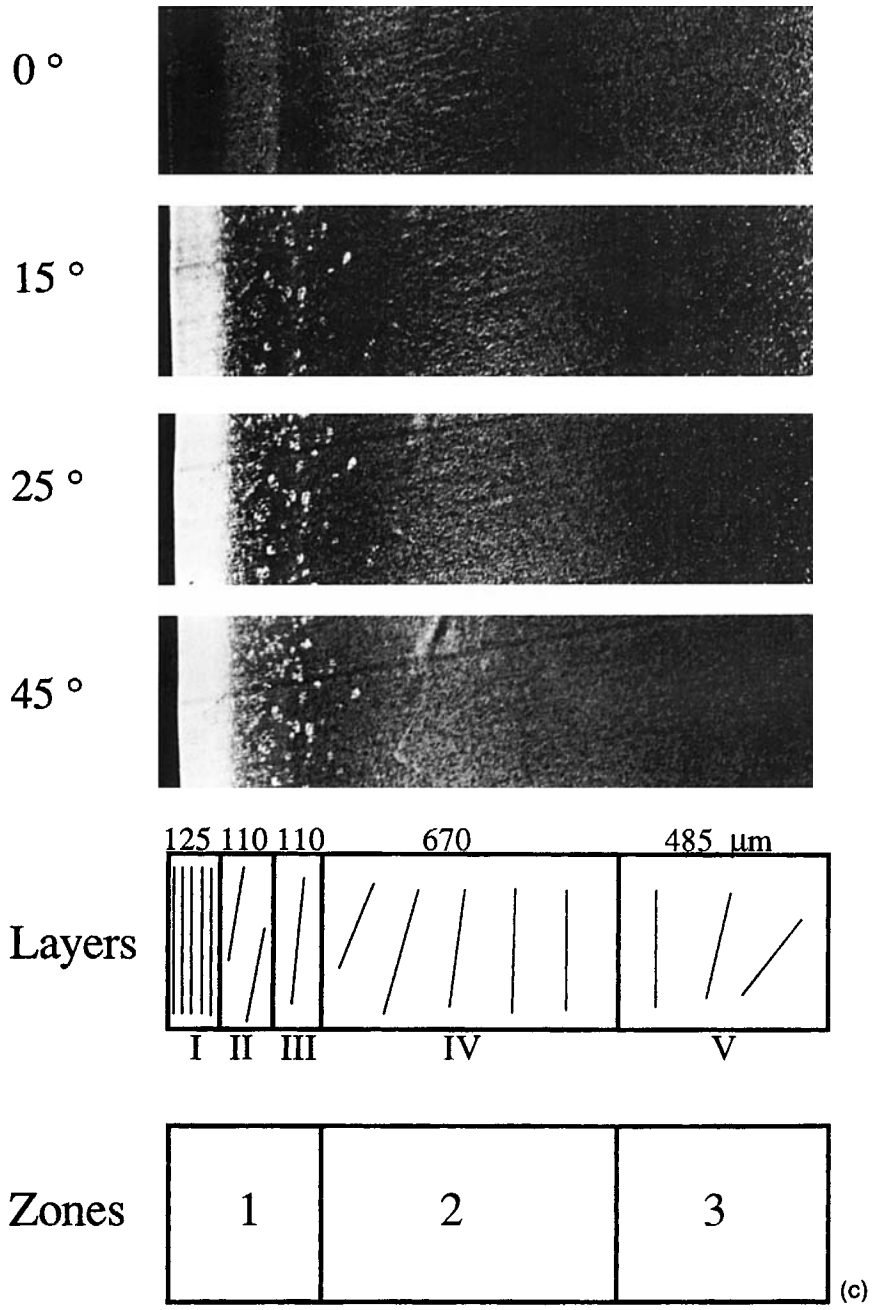

Figure 5 (*Continued from the previous page*)

Comparison of Morphology of Injection-molded Samples

In Figure 5(b), micrographs of PP-Px are presented at the same cross polar angles as in Figure 5(a). The region where the skin is seen in PP is separated into two regions. A very thin layer at the surface, Ia, shows similar birefringence to the skin in PP. A second layer, Ib, is 135 μm thick and has a transcrystalline texture. It is not highly oriented. Layer II, faintly observable in the micrographs, is 90 μm thick and is analogous to Layer II of PP. Layer III is 45 μm thick and closely resembles Layer III of PP. Layer IV in PP-Px is thinner than in PP, and Layer V, the isotropic core, is much thicker than in PP. This thicker isotropic core is due to the lower crystallization temperature of PP-Px, which allows more time for relaxation before crystallization.

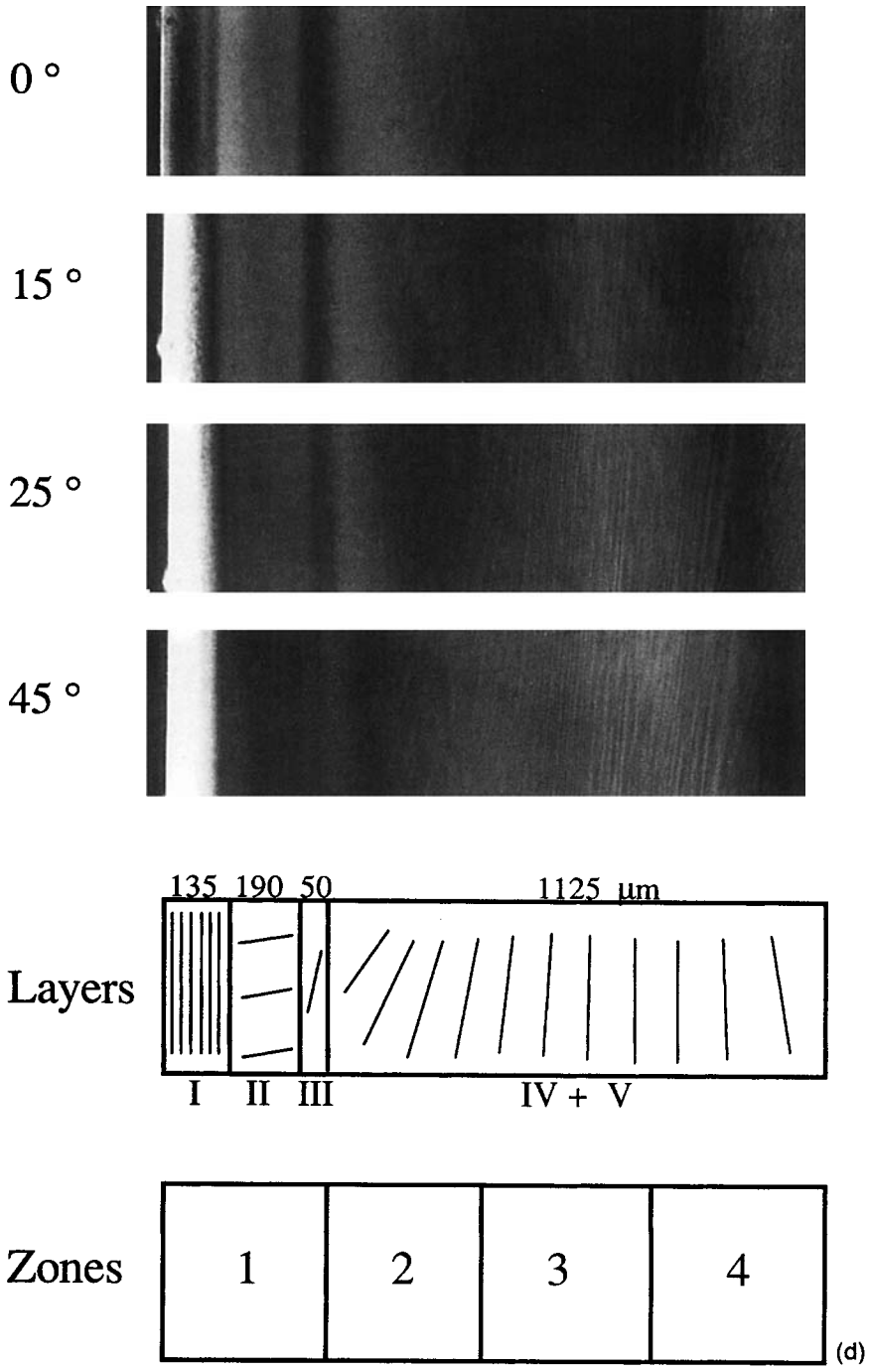

Figure 5 (*Continued from the previous page*)

Micrographs of PP-Tc are presented in Figure 5(c). Layers I–III are virtually the same as in PP. Layer IV is much thicker than in PP, indicating that the melt orientation is retained further in from the mold wall. In Layers IV and V, the texture of the sample is also much finer than is PP, indicative of nucleation. In this sample, the core, Layer IV, is not isotropic but retains some of the melt orientation due to the higher crystallization temperature.

The micrographs of PP-Md [Fig. 5(d)] reveal a very highly nucleated structure where individual spherulites are indistinguishable. Layers I and II show similar orientation to the corresponding layers of PP. Layer III is also like Layer III of PP in that

it does not show any preferred orientation. There is no isotropic core; instead, a gradient in orientation extends to the center of the sample through the region designated Layer (IV + V). Layer (IV + V) not only shows a high degree of orientation, but even a striated texture in the center of the layer where the average chain axis orientation is parallel to the injection direction.

Modulus Measurements

The bottom schematic in Figure 5(a)–(d) depicts the approximate size and location of the sections used to determine the temperature-dependent modulus. Some individual layers were too thin, 100 μm or less, to test individually, so the sample was divided into three or four zones for testing. The results are presented in Figure 6(a)–(d).

In Figure 6(a), the modulus of each of the three PP zones is shown. Zone 3, the core, had the highest modulus and it was comparable to the modulus of the compression-molded PP. The modulus of the anisotropic Zones 1 and 2 was about the same and was lower than that of Zone 3, especially in the temperature range of the HDT, even though the chains were preferentially oriented in the injection direction. The modulus of specimens taken from the three zones of PP-Px is shown in Figure 6(b). As with PP, the almost isotropic core, Zone 3, had the highest modulus and the only significant difference between PP and PP-Px was the much lower modulus of Zone 2 in PP-Px. The temperature-dependent modulus of the three PP-Tc zones was virtually the same [Fig. 6(c)]. At RT, the modulus of the zones was higher than the compression-molded modulus; yet, the modulus differences disappeared in the range of the HDT. In Figure 6(d), the modulus of Zones 2, 3, and 4 of PP-Md was about the same, with Zone 3 being slightly higher. Zone 3 was also the region where the striated texture in the micrographs was most intense. The modulus of these zones was much higher than the compression-molded value. The modulus of Zone 1 was significantly lower than the other zones and comparable to the compression-molded specimen.

Estimation of HDT using a Composite Beam Approach

To accommodate the anisotropic gradient structure through the thickness, the HDT test bar was modeled as a series of parallel elements. Using Zone 3 (or 4) as a reference, the thickness of each of the other zones was converted to an equivalent thickness that would have the same modulus as the reference

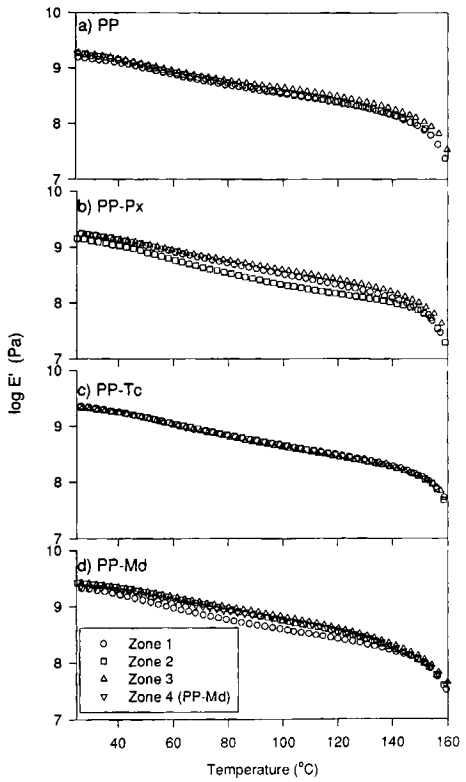

Figure 6 Temperature dependence of the modulus of each zone from the HDT bars determined by DMTA at 1 Hz: (a) PP; (b) PP-Px; (c) PP-Tc; (d) PP-Md.

zone. The effective thickness, b_{eff}, was then defined as the sum of the equivalent thicknesses:

$$b_{\text{eff}} = \sum m_i b_i \tag{3}$$

where $m_i = E_{\text{zone}i}/E_{\text{zone3}}$ and b_i is the original thickness of the zone.

Each modulus curve was fit with a fourth-order polynomial and the modulus ratio, m_i, was calculated at intervals of 2°C to obtain b_{eff} as a function of temperature. With the gradient cross section represented by a uniform bar with thickness b_{eff} and modulus of Zone 3 (or 4), $\mathcal{D}(T)$ was then calculated from $b_{\text{eff}}(T)$ and $E_{\text{zone3}}(T)$ using eq. (2). With the 15°C temperature correction for the frequency, the calculated deflection curves are presented in Figure 7. The temperature at which the HDT criterion is achieved varies among the samples. The curves show a separation at the HDT criterion from a low of 113°C for PP-Px to a high of 124°C for PP-Md. The intermediate values of PP and PP-Tc are 116 and 122°C, respectively. The calculation reproduces the higher HDT of the nucleated samples as well the slight decrease seen of PP-Px. These values are significantly higher than the measured values. There

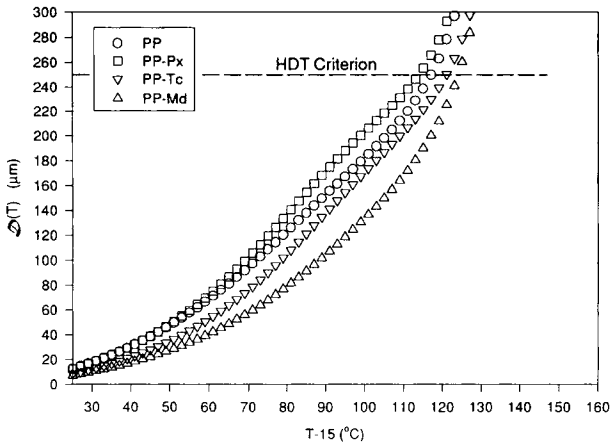

Figure 7 Calculated deflection as a function of temperature using injection-molded modulus values. HDT criterion given at 250 μm.

exist several possible reasons for this difference: Some error could occur in using only the midregion of the HDT bar in the modulus measurements, as the gradient structure would not be the same along the entire length of the mold. Also, the layered structure does not incorporate edge effects at the top and the bottom of the bar. However, the calculated values are in very good agreement with literature values of similar polypropylene compounds prepared under similar molding conditions, Table I.[1] This could indicate an error in the actual measurement of the HDT values.

CONCLUSIONS

In summary, no correlation was found between the HDT of various polypropylenes and the modulus of isotropic samples in the temperature range of the HDT. Instead, the HDT of injection-molded bars was directly related to the anisotropic morphology gradient produced by the injection process. The extent of orientation was determined by the crystallization temperature. The higher crystallization temperature of nucleated polypropylene resulted in increased retention of melt orientation. This increase in orientation correlated with an increase in the high-temperature modulus and therefore with an increase in the HDT. Modeling the HDT test as a three-point bend test and incorporating the anisotropic morphology and modulus gradients of the injection-molded samples successfully predicted the differences seen in the measured HDT values.

The authors thank the Ferro Corp. for their generous support of this work.

REFERENCES

1. M. Fujiyama and T. Wakino, *J. Appl. Polym. Sci.*, **42,** 2739 (1991).
2. S. S. Katti and J. M. Schultz, *Polym. Eng. Sci.*, **22,** 1001 (1982).
3. T. K. Kwei, H. Schonhorn, and H. L. Frisch, *J. Appl. Phys.*, **38,** 2512 (1967).
4. Manufacturer's Technical Data Sheet, CR-05, Polyvel Inc.
5. Manufacturer's Technical Data Sheet, Vantalc 6h, R. T. Vanderbuilt Co.
6. Manufacturer's Technical Data Sheet, Millad 3940, Milliken Chemical.
7. ASTM D 648.
8. B. Wunderlich, *Macromolecular Physics,* Academic Press, New York, 1973, Vol. 1.
9. F. Rybnikar, *J. Appl. Polym. Sci.*, **38,** 1479 (1989).
10. R. F. Boyer, *Encyclopedia of Polymer Science and Technology,* Wiley, New York, 1977, Supp. Vol. II, p. 788.
11. Z. Tadmor, *J. Appl. Polym. Sci.*, **18,** 1753 (1974).
12. H. Mavridis, A. N. Hrymak, and J. Vlachopoulos, *J. Rheol.*, **32,** 639 (1988).

Received October 13, 1995
Accepted November 14, 1995